RC24583 (W0806-041) June 11, 2008
Materials Science

IBM Research Report

Undercooling and Microhardness of Pb-free Solders on Various UBMs

Moon Gi Cho[1], Sung K. Kang[2], Hyuck Mo Lee[1]*

[1]Department of Materials Science and Engineering
Korea Advanced Institute of Science and Technology
Gusung-Dong 373-1, Yusung-Gu
Deajon 305-701
Republic of Korea

[2]IBM Research Division
Thomas J. Watson Research Center
P.O. Box 218
Yorktown Heights, NY 10598

*Corresponding author (e-mail: hmlee@kaist.ac.kr, Tel: +82-42-869-3334, Fax: +82-42-869-3310)

Research Division
Almaden - Austin - Beijing - Cambridge - Haifa - India - T. J. Watson - Tokyo - Zurich

Abstract

The undercooling behavior of pure Sn, Sn-0.7Cu, Sn-3.5Ag and Sn-3.8Ag-0.7Cu solder alloys was observed in terms of various under bump metallurgies (UBMs). Four different UBMs (electroplated Cu, electroplated Ni, electroless Ni-P and electroless Ni-P/immersion Au) were employed. The amount of the undercooling of Pb-free solder alloys was reduced when reacted with electroplated Cu UBM and Ni-based UBMs.The Ni-based UBMs were more effective than Cu UBM in reducing the undercooling of Pb-free solders. When Ni_3Sn_4 was formed during the interfacial reactions with Ni-based UBMs, the reduction of undercooling was significant, especially for pure Sn and Sn-3.5Ag. The effects of UBMs on the undercooing of Pb-free solder alloys are discussed by comparing intermetallic compounds (IMCs) formed during interfacial reactions with UBMs. In addition, the microstructural changes as well as the microhardness of four solders with or without UBMs are discussed, which could be related to their undercooling behaviors.

Key Words: Undercooling, Pb-free solder, UBM, Intermetallic compounds

1. Introduction

Sn-based, near eutectic binary or ternary solder alloys are the promising Pb-free candidates to replace Pb-containing solders in electronic packaging, which include Sn-0.7Cu, Sn-3.5Ag and Sn-3.8Ag-0.7Cu (in wt.% unless specified otherwise). The extensive searches for Pb-free solder alloys in last several years were conducted to produce reliable Pb-free solder joints.[1-5] Since most Sn-based Pb-free solders consist of more than 90 wt.% Sn and minor amounts of alloying additions such as Cu and Ag, their physical, chemical and mechanical properties are heavily influenced by the properties of pure Sn.[5] The undercooling behavior of Sn-based Pb-free solders is also one of such propensities. Undercooling is defined as the difference between melting and solidification temperature during heating and cooling, respectively. When an appreciable amount of undercooling is observed, the solidification does not occur at the melting point, but at a relatively lower temperature. This is attributed to the difficulty in nucleating a solid phase from a liquid phase.

In case of the pure Sn without any impurities, the maximum undercooling

observed was 107~120K.[6,7] The amount of undercooling in Sn-based Pb-free solders reported by recent works is about 30°C, which is much larger than the undercooling observed in Pb-rich solders.[8-10] The large amount of undercooling in Ag-containing Pb-free solders such as Sn-3.5Ag and Sn-3.8Ag-0.7Cu can cause and accelerate the formation of large Ag_3Sn plates, because it provides a longer growth time for the proeutectic Ag_3Sn plates in a supersaturated liquid during cooling.[8,9] In addition, it was reported that the amount of undercooling in Sn-based solders is inversely proportional to a sample size, suggesting that a smaller solder joint would show a larger undercooling.[11-13] Moreover, this large undercooling can also affect the microstructures of Sn-rich solder alloys as well as their mechanical properties. It was also reported that when the undercooling amount of a solder is different for different solder volumes, the microstructures and mechanical properties such as tensile strength are changed.[14] Since Sn-rich solders are expected to be used in flip-chip solder joints with a small solder volume, it is very important to understand and control the undercooling behavior of Sn-rich solders.

In order to reduce the undercooling of Sn-based solder alloys, it has been suggested to promote the nucleation of β-Sn phases by modifying solder composition

and/or by adding impurity elements. It was reported that the undercooling of Sn-Ag-Cu and Sn-Cu solders was significantly reduced by adding minor alloying elements, such as Zn, Co and Fe.[10,12,15,16] Most reports for the undercooling of Pb-free solders were limited to the bulk properties only. The effect of a wettable surface, such as under bump metallurgy (UBM) in flip-chip applications was not extensively investigated. A wettable surface would be effective in reducing the undercooling of Sn-based solders because it offers a heterogeneous nucleation site in solidifying the β-Sn phase. Only a limited study has been reported for the beneficial effect of a wettable surface on reducing the undercooling of Sn-rich solders.[12] In this study, we have investigated the undercooling behaviors of pure Sn, Sn-0.7Cu, Sn-3.5Ag and Sn-3.8Ag-0.7Cu solder alloys during the interfacial reactions with various UBMs. Four different UBMs (electroplated Cu, electroplated Ni, electroless Ni-P and electroless Ni-P/immersion Au) were employed. The effects of UBMs on the undercooing of Pb-free solder alloys were discussed by comparing intermetallic compounds (IMCs) formed during the interfacial reaction with UBMs. In addition, the changes in microstructure and microhardness of four solders on UBMs were investigated.

2. Experimental Procedures

The solder compositions used in this experiment are pure Sn, Sn-3.5Ag (SA), Sn-0.7Cu (SC) and Sn-3.8Ag-0.7Cu (SAC), which were commercially produced. Four different types of the UBMs employed were electroplated Cu, electroplated Ni, electroless Ni(6wt.%P) and electroless Ni(6wt.%P)/immersion Au (0.1μm). Approximately, the same substrate size (1mm X 1mm) of different UBMs and solder weight (4.8mg, d=1050μm) were used to eliminate any effects due to the variation in solder volume or substrate area. Interfacial reaction experiments were conducted by reflowing the same amount of a solder on a substrate on a hotplate at 260°C for 10sec with RA-type flux. Subsequently, the differential scanning calorimetry (DSC) experiments were performed in a Diamond DSC calorimeter (Perkin-Elmer, Inc.), which was heated and cooled at the rate of 6°C/min under a nitrogen atmosphere with the substrate plus solder.

After DSC experiments, the interface of solders and substrates was revealed on its cross section by mounting and polishing. Optical microscopy (OM) and scanning electron microscopy (SEM) were used to characterize the microstructures and the IMCs.

The back-scattered electron mode of SEM was used to observe the IMCs, and energy-dispersive X-ray spectroscopy (EDS).

Microhardness tests were performed to compare the Vickers hardness number (VHN) of samples that underwent the same thermal profile in DSC. The load of hardness tests was 10g and loading time was 5sec. The VHN was reported as an average value of ten indentations or more.

3. Results and Discussion

Undercooling of Pb-free Solders on Various UBMs

Figure 1 depicts the thermal profile recorded during heating and cooling of a Pb-free solder. Peak and onset temperatures in heating and cooling curves were measured from Fig. 1. Generally, the amount of undercooling can be estimated by using either onset-to-onset (T_1-T_2) or peak-to-peak method. In this study, the onset-to-onset method was used to estimate the amount of undercooling since it describes better the physical process occurring during melting and solidification.

Table 1 summarized the DSC results obtained from four solder alloys with or without UBMs. For each solder, the onset and peak temperatures of the thermal profile were recorded with four different UBMs. In addition, the difference of onset temperatures was evaluated as the amount of undercooling of each case. For the bulk solder alloys without UBMs, the amount of undercooling is not much sensitive to their compositions, only varying from 25 to 30°C. The undercooling of pure Sn (31.2°C) was only reduced 1 or 2°C by adding 0.7Cu or 3.5Ag to its binary system, and about 5°C by adding 0.7Cu and 3.8Ag together. However, the undercooling of pure Sn was significantly reduced by 10 to 20°C when pure Sn was reacted with four different UBMs. This was also true with other Pb-free solders (SC, SA and SAC), as shown in Table 1. The reduction of the undercooling of Sn-rich solder alloys when reacted with various UBMs is attributed to a wettable surface of UBMs, which facilitates a heterogeneous nucleation of β-Sn phase during its solidification, consistent with the previous observation (Ref. 12).

A portion of the thermal profile recorded during heating and cooling of four solders on each UBM (shown in dotted line of Fig. 1) was rescaled and compared each other, as collected in Fig. 2. In case of pure Sn and SA, a decrease of 20°C on Ni-based

UBMs was obtained, while 10°C on Cu UBM. Moreover, it is interesting to note that the heating onset temperatures (T_1) of pure Sn and SA decreased on Cu UBM, while very little changes observed with Ni-based UBMs. Nevertheless, the onset temperatures (T_2) during solidification of pure Sn and SA on Ni-based UBMs were higher than on Cu UBM by about 10°C. In case of SC and SAC, the amount of the undercooling reduced on UBMs was about 10°C, independent on the type of UBMs (Cu vs. Ni-based UBMs). In addition, the undercooling of each solder changed by the reaction with three types of Ni-based UBMs (electroplated Ni, electroless Ni(P), Ni(P)/immersion Au) was almost similar.

IMCs Formation during DSC

As discussed above, a significant reduction of the undercooling (10~20°C) was observed when pure Sn or Sn-based solders were reacted on various wettable surfaces of Cu and Ni UBMs. In addition, the degree of the undercooling reduction was found to be different depending on solder alloys and UBMs. The undercooling of pure Sn and SA was reduced much more on Ni-based UBMs than on Cu UBM, while in case of SC and SAC, the difference was not very significant.

In order to explain the effects of Ni vs. Cu UBMs on the undercooling behaviors of Sn-rich solders, the IMCs formed at the interface between solders and UBMs during DSC were identified by SEM and EDS. Figure 3 exhibits representative SEM images of the interface between four solders and four UBMs. IMCs formed at the interface were analyzed by EDS to obtain the information on their compositions. The scallop-like Cu_6Sn_5 IMCs were identified commonly at the interface between all solders and Cu UBM, and Cu_3Sn IMCs were occasionally found.

However, IMCs formed on Ni-based UBMs were varied with the type of solder alloys. The needle-like and chucky Ni_3Sn_4 IMCs in case of pure Sn and SA were observed on all Ni-based UBMs. It was known that the Au layer in Ni(P)/immersion Au UBM did not form any IMCs with a solder during reflow, but fully dissolved into a solder because the very thin layer of immersion Au was plated.[17] In this study, any Au-containing IMCs was not observed, but only Ni_3Sn_4 at the interface between pure Sn and SA and Ni(P)/immersion Au UBM. Merely, the spalled N_3Sn_4 IMCs were locally observed on Ni(P)/Au UBM, different from other Ni-based UBMs. IMCs formed at the interface between SC and SAC and Ni-based UBMs were identified as the ternary Sn-Cu-Ni compounds, consisting of Sn (47~49 at.%), Cu (16~19 at.%) and Ni (32~34

at.%). The morphology of the ternary Sn-Cu-Ni compounds was thin rod-shape. The ternary IMCs appeared to be $(Cu,Ni)_6Sn_5$ in the view of their atomic ratios, but their morphology suggests that IMCs may be Ni_3Sn_4. By the way, it was reported that when Pb-free solders with Cu of more than 0.4 wt.%, the $(Cu,Ni)_6Sn_5$ IMC was formed at the interface even though solders were reacted with Ni-based UBMs during reflow.[18] It was also reported that the morphology of $(Cu,Ni)_6Sn_5$ was thin rod-shape, different from the scallop-like Cu_6Sn_5.[19] In our study, considering the Cu content (0.7 wt.%) of SC and SAC, the atomic ratios and their morphology of the ternary Sn-Cu-Ni IMCs, the IMCs are regarded as $(Cu,Ni)_6Sn_5$, not Ni_3Sn_4 type.

In relating the results of undercooling with the interfacial reactions, it is suggested that Ni-Sn type IMCs are more effective than Cu-Sn type IMCs in reducing the amount of undercooling observed with Sn-rich solder alloys. A decrease of about 20°C in undercooling was obtained when pure Sn and SA were reacted on Ni UBMs, forming Ni-Sn IMCs, while a reduction of about 10°C in undercooling was attained when Cu-Sn IMCs were formed with pure Sn and SA on Cu UBM, and SC and SAC on Cu and Ni UBMs.

Microstructures

Microstructural changes accompanied with the changes of undercooling were also investigated by OM. Figure 4 are the typical OM images of solders far inside from the interface, which were solidified at the cooling rate of 6°C/min during DSC. For pure Sn, a large grain structure was observed in a bulk solder with Ni_3Sn_4 or Cu_6Sn_5 IMCs probably precipitated from the dissolved Ni or Cu atoms during the interfacial reactions. Especially, the microstructure of pure Sn with Cu UBM was very similar to those of Sn-Cu solders, consisting of Sn dendrite (light contrast) and the Sn-Cu eutectic phases (dark contrast). For SC, SA and SAC, the β-Sn dendrites and the eutectic phase (a mixture of the intermetallic particles such as Cu_6Sn_5 in SC, Ag_3Sn in SA, and Ag_3Sn and Cu_6Sn_5 in SAC), were observed in three bulk solders. The microstructures of three Sn-based solders reacted with Cu or Ni-based UBMs also consisted of β-Sn dendrites and the eutectic phase, but they were much coarser than those of the bulk solders without UBMs. Namely, the β-Sn dendrites on Cu or Ni-based UBM were much larger than those in the bulk solders, and the eutectic phases also formed a thicker continuous network.

Xiao et al. reported the undercooling and microstructures changed when the

size of a cast solder was varied.[14] They found that a large volume exhibited a smaller undercooling and coarser microstructure (large β-Sn dendrites and a thick network of the eutectic phases) than the solder with a smaller volume even though the same solder composition of Sn-3.8Ag-0.7Cu was used.[14] In our study, Cu or Ni atoms can dissolve from UBMs into three Sn-based solders during the interfacial reactions, and the volume fraction of the eutectic phase can increase as the amount of alloying elements increases. Actually, when the volume fraction of the eutectic phase in the bulk SC, SA and SAC solders is compared, it increased in the order of SC, SA and SAC. However, the increase in the amount of alloying elements did not influence the size of β-Sn dendrites. Namely, the β-Sn dendrites of SC, SA and SAC were similar in amount, as shown in Fig. 4. Therefore, the microstructural changes associated with the interfacial reactions of SC, SA and SAC on Cu or Ni-based UBMs (larger β-Sn dendrites and the thicker eutectic phases) would rather be due to the decrease in undercooling than the compositional changes of the solders due to Cu or Ni atoms dissolved from UBMs.

Furthermore, when the undercooling of Sn-based solders is reduced by the interfacial reactions with UBMs, the nucleation and growth of solidifying phases occur at a higher temperature than those without UBMs by 10 or 20°C. In general, the

solidifying grain can grow faster as temperature is higher, and then a large grain structure can be formed. This also seems to explain why the microstructures of Sn-based solders with UBMs are much coarser than those of the bulk solders without UBMs.

Microhardness Measurement

The hardness tests were performed to observe the change of mechanical properties associated with the microstructure changes. The bulk solders and solders reacted on electroplated Cu and electroplated Ni during DSC experiment were employed for their microhardness measurement, because other UBMs did not produce any significant difference in their microstructures. Figure 5 is the microhardness results as a function of alloy composition and the type of UBMs. Each sample was exposed to the same thermal profile during DSC measurements, solidified at the rate of 6°C/min. In general, the hardness of Sn-based solders strongly depends on the alloying elements; the more alloying elements there are, the higher the hardness is. This is attributed to the fact that the volume fraction of the eutectic phase increases as there are more alloying elements in solder. In this study, the same trend was confirmed; the average hardness value increases in order of pure Sn, SC, SA and SAC, as shown in Fig. 5.

However, when the solders reacted with UBMs, the microhardness changes observed were different in pure Sn and three Sn-based solders (SC, SA and SAC). The microhardness of pure Sn increased after the reaction with UBMs. The VHN of bulk pure Sn was 8.9, while those of pure Sn on Cu and Ni UBM were 10.6 and 10.2, respectively. But, for other three Sn-based solders, the microhardness decreased after the reaction with UBMs. For example, the VHN of bulk SAC was 15.9, but 14.2 on Cu UBM and 14.0 on Ni UBM. In other words, the hardness of pure Sn increased by 10~15% after the reaction with UBMs, while that of SC, SA and SAC solders decreased by about 10%. In addition, the VHNs of each solder on Cu and Ni UBM were almost similar.

The hardness increase in pure Sn after reacted with either Cu or Ni UBM during DSC run can be understood by noting dissolution of Cu or Ni atoms for the corresponding UBM and then forming IMC particles in the solder matrix to promote precipitation hardening. However, the hardness decrease in SC, SA and SAC solders reacted on Cu or Ni UBM does not follow the general behavior of precipitation hardening. This may be explained by the microstructural coarsening observed in three Sn-based solders after reacted with UBMs; the β-Sn dendrites and the eutectic IMCs

dispersed in Sn matrix were coarser than those of the bulk solders. As discussed earlier, the microstructural coarsening in the solders reacted with UBMs is attributed to the decrease in the undercooling of each corresponding solder alloy. Therefore, the decrease in hardness of SC, SA and SAC after reacted with UBMs is attributed to the reduction of undercooling on UBMs.

4. Summary

The undercooling behavior of pure Sn, Sn-0.7Cu, Sn-3.5Ag and Sn-3.8Ag-0.7Cu solder alloys was observed in terms of various UBMs such as electroplated Cu, electroplated Ni, electroplated Ni(P) and Ni(P)/immersion Au. It was found that the presence of a wettable surface such as Cu or Ni UBMs can significantly reduce the undercooling of bulk Sn-rich solders. A decrease of about 20°C in undercooling was obtained when Ni_3Sn_4 IMCs were formed during interfacial reactions between pure Sn and SA and Ni-based UBM. About 10°C reduction in undercooing was observed when Cu_6Sn_5 or $(Cu,Ni)_6Sn_5$ IMCs were formed between pure Sn and SA on Cu UBM, and SC and SAC on Cu and Ni-based UBM.

Changes of the microstructure and hardness in four solders with or without UBMs were also found to be affected by their undercooling behaviors. For pure Sn, a large grain structure of the bulk solder changed to the Sn matrix with IMCs (Cu_6Sn_5 or Ni_3Sn_4) after the reaction with UBMs, and consequently a 10~15% increase of the hardness was obtained. For Sn-0.7Cu, Sn-3.5Ag and Sn-3.8Ag-0.7Cu, the unique microstructures (β-Sn dendrite and eutectic phases) of bulk solders became much coarser after the reaction with UBMs due to the corresponding reduction in the undercooling, and consequently about 10% decrease of the hardness was obtained.

Acknowledgements

We appreciate very much Drs. Hae Jin Kim and Jin Bae Lee at the Korea Basic Science Institute (KBSI) for their work on DSC measurements as well as Han-Na Park in KBSI for the SEM observation and EDS analysis.

References

1. J. Bath, C. Handwerker, and E. Bradley, *Circ. Assemb.* 11, 45 (2000).

2. I.E. Anderson, J.C. Foley, B.A. Cook, J. Harringa, R.K. Terpatra, and O. Unal, *J. Electron. Mater.* 29, 1050 (2001).

3. K.J. Puttlitz, *Handbook of Lead-Free Solder Technology for Microelectronic Assemblies*, ed. K.J. Puttlitz and K.A. Stalter (New York: Marcel Dekker, Inc., 2004), pp. 239–280.

4. S.W. Jeong, J.H. Kim, and H.M. Lee, *J. Electron. Mater.* 33(12), 1530 (2004).

5. S.K. Kang, P. Lauro, D.Y. Shih, D.W. Henderson, and K.J. Puttlitz, *IBM Journal of Res.&Dev.* 49(4/5), 606 (2005).

6. B. Vonnegut, *J. Colloid. Sci.* 3, 563 (1948).

7. G.M. Pound and V.K. LA Mer, *J. Amer. Chem. Soc.* 74, 2323 (1952).

8. S.K. Kang, W.K. Choi, D.-Y. Shih, D.W. Henderson, T. Gosselin, A. Sarkhel, C. Goldsmith, and K.J. Puttlitz, *Proceedings of 53rd Electronic Components and Technology Conference* (Piscataway, NJ: IEEE, 2003), pp. 64-70.

9. L.P. Lehman, R.K. Kinyanjui, L. Zavalij, A. Zribi, and E.J. Cotts, *Proceedings of 53rd Electronic Components and Technology Conference* (Piscataway, NJ: IEEE, 2003), pp. 1215-1221.

10. S.K. Kang, D.-Y. Shih, D. Leonard, D.W. Henderson, T. Gosselin, S.-I. Cho, J. Yu, and W.K. Choi, *JOM* 56(6), 34 (2004).

11. R. Kinyanjui, L.P. Lehman, L. Zavalij, and E. Cotts, *J. Mater. Res.* 20(11), 2914 (2006).

12. S.K. Kang, M.G. Cho, P. Lauro, and D.-Y. Shih, *Proceedings of 57th Electronic Components and Technology Conference* (Piscataway, NJ: IEEE, 2007), pp. 1597-1603.

13. S.K. Kang, M.G. Cho, P. Lauro, and D.-Y. Shih, *J. Mater. Res.* 22(3), 557 (2006).

14. Q. Xiao, L. Nguyen, and W.D. Armstrong, *J. Electron. Mater.* 34(5), 617 (2005).

15. K.S. Kim, S.H. Huh, and K. Suganuma, *Microelectron. Reliab.* 43, 259 (2002).

16. I. de Sousa, D.W. Henderson, L. Party, S.K. Kang, and D.-Y. Shih, *Proceedings of 56th Electronic Components and Technology Conference* (Piscataway, NJ: IEEE, 2006), pp. 1454-1461.

17. Y.-D. Jeon, S. Nieland, A. Ostmann, H. Reichl, and K.-W Paik, *J. Electron. Mater.* 32(6), 548 (2003).

18. C.E. Ho, S.C. Yang, and C.R. Kao, *J. Mater. Sci.: Mater. Electron*. 18, 155 (2007).

19. S.-W. Chen and C.-H Wang, *J. Mater. Res.* 21(9), 2270 (2006).

Table 1. DSC results for undercooling of pure Sn, Sn-0.7Cu (SC), Sn-3.5Ag (SA) and Sn-3.8Ag-0.7Cu (SAC) with or without UBMs.

composition (wt.%)	UBMs	onset temp. (heating) (T_1)	onset temp. (cooling) (T_2)	ΔT (T_1-T_2)	peak temperature*
pure Sn	-	232.3°C	201.1°C	**31.2**	234 (H), 201.2 (C)
	on Cu	227.7°C	210.6°C	**17.1**	229.8 (H), 210.5 (C)
	on Ni	232.1°C	223.0°C	**9.1**	234.9 (H), 222.8 (C)
	on NiP	231.6°C	219.2°C	**12.4**	235.0 (H), 218.9 (C)
	on NiP/Au	230.2°C	219.6°C	**10.6**	234.3 (H), 219.4 (C)
Sn-0.7Cu (SC)	-	229.6°C	200.3°C	**28.8**	230.3 (H), 202.3 (C)
	on Cu	227.7°C	206.5°C	**21.2**	229.9 (H), 206.5 (C)
	on Ni	227.5°C	208.8°C	**18.7**	230.6 (H), 208.7 (C)
	on NiP	227.6°C	208.0°C	**19.6**	230.4 (H), 207.9 (C)
	on NiP/Au	226.9°C	209.0°C	**17.9**	230.0 (H), 208.9 (C)
Sn-3.5Ag (SA)	-	222.1°C	192.5°C	**29.6**	223.7 (H), 192.5 (C)
	on Cu	218.0°C	201.9°C	**16.1**	220.5, 222.4 (H), 201.7 (C)
	on Ni	221.5°C	210.6°C	**10.9**	224.7 (H), 210.2 (C)
	on NiP	221.4°C	209.7°C	**11.7**	225.5 (H), 209.3 (C)
	on NiP/Au	220.1°C	207.7°C	**12.4**	223.8 (H), 207.4 (C)
Sn-3.8Ag-0.7Cu (SAC)	-	218.5°C	193.9°C	**24.6**	219.6 (H), 193.9 (C)
	on Cu	217.9°C	197.2°C	**20.7**	220.5 (H), 197.2 (C)
	on Ni	218.1°C	200.7°C	**17.4**	221.6, 219.7 (H), 200.5 (C)
	on NiP	218.0°C	202.4°C	**15.6**	220.9 (H), 202.3 (C)
	on NiP/Au	217.0°C	202.4°C	**14.6**	221.1 (H), 202.1 (C)

* H stands for heating and C for cooling.

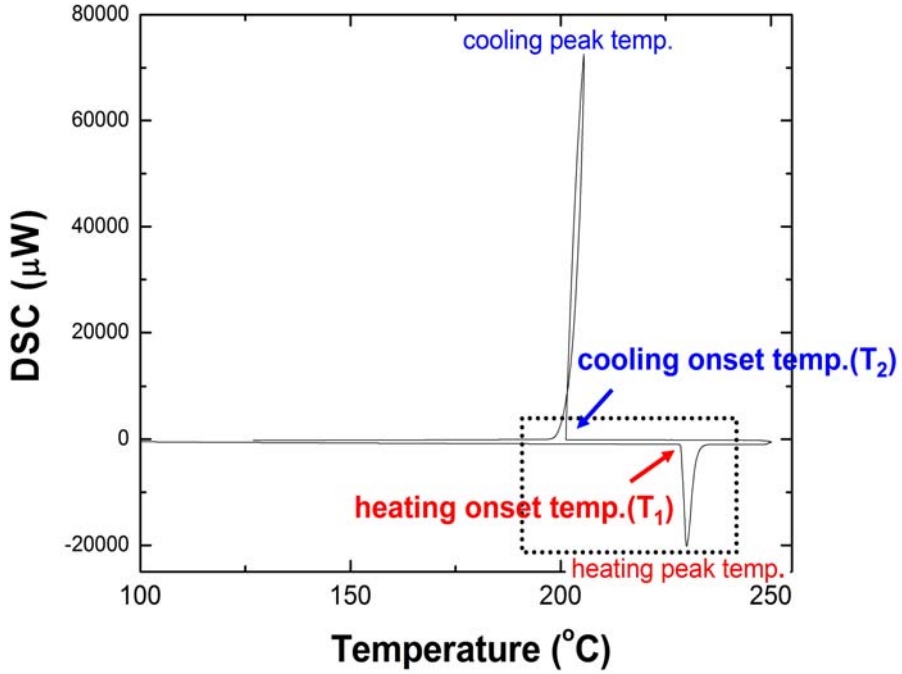

Figure 1. A typical DSC thermal profile recorded during heating and cooling of a Pb-free solder.

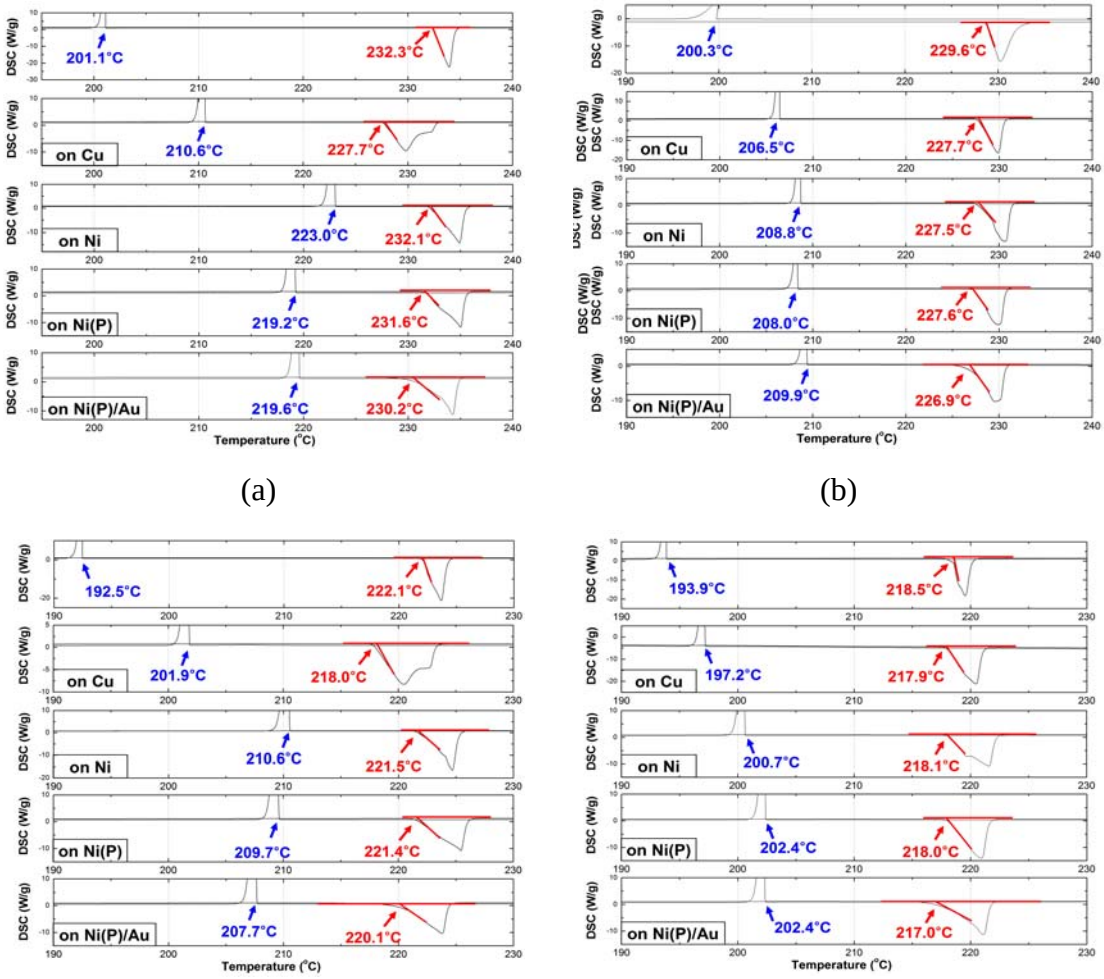

Figure 2. A part of the DSC thermal profile recorded during heating and cooling of (a) pure Sn, (b) Sn-0.7Cu, (c) Sn-3.5Ag and (d) Sn-3.8Ag-0.7Cu with or without UBMs (the enlarged portion shown inside the dotted box of Fig. 1).

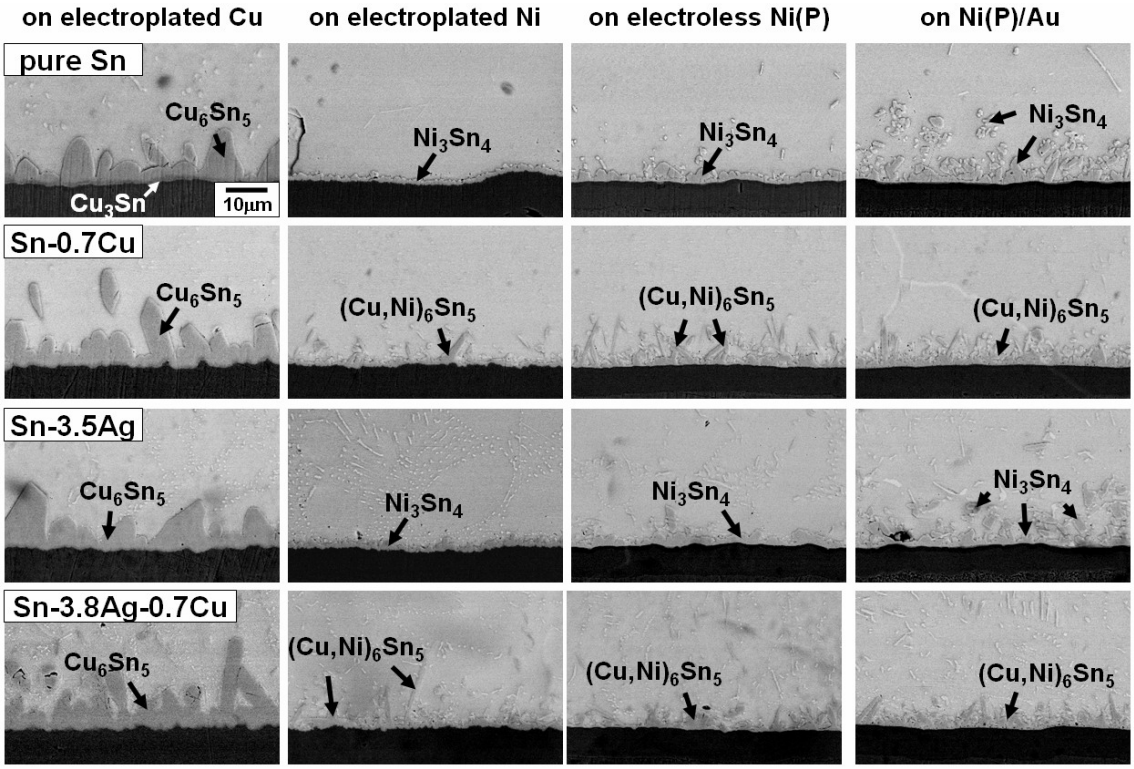

Figure 3. SEM images of the interface area between each solder and various UBMs (electroplated Cu, electroplated Ni, electroless Ni(P), Ni(P)/immersion Au) after DSC measurement.

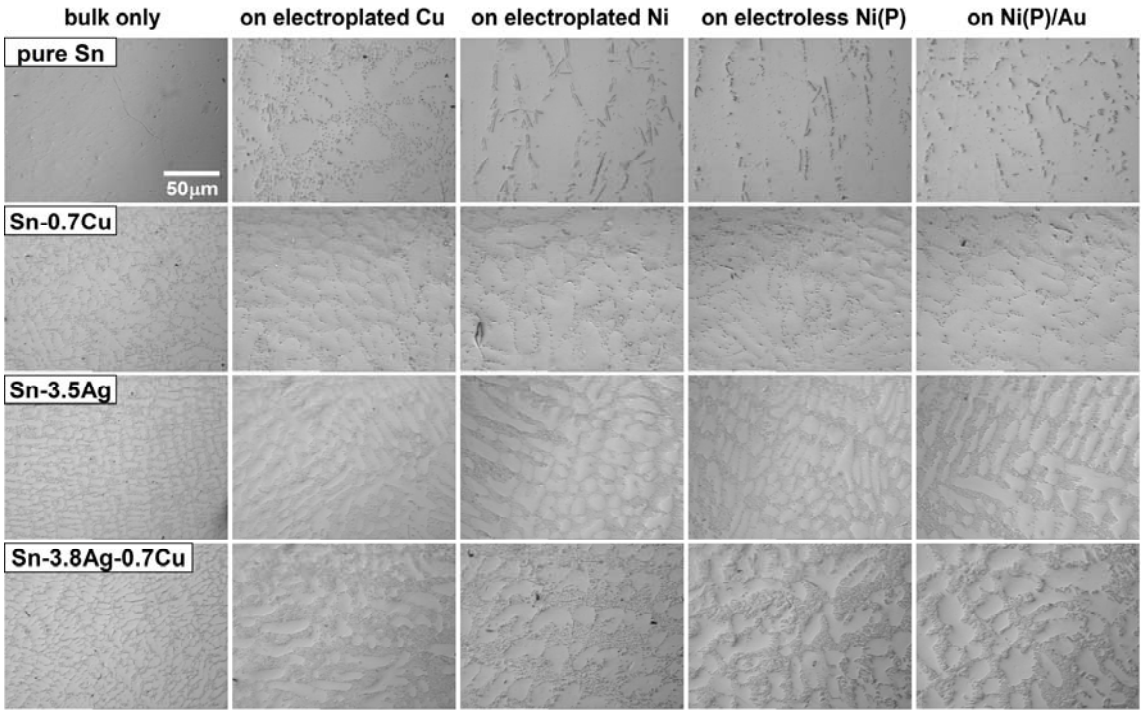

Figure 4. OM images inside the four solders solidified at a cooling rate of 6°C/min during DSC.

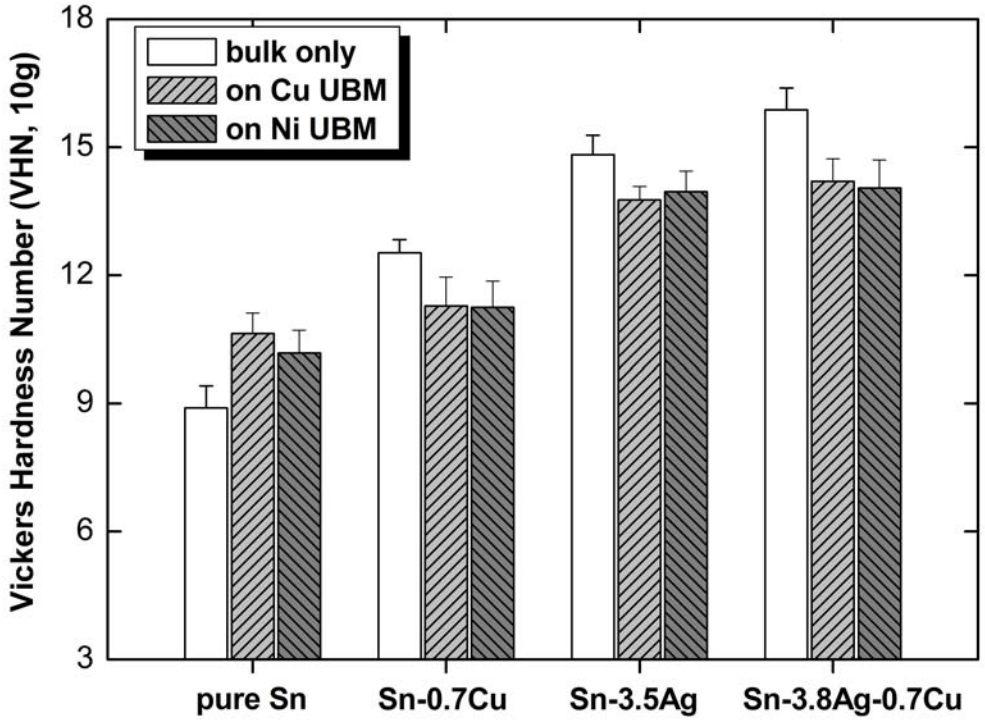

Figure 5. Microhardness results of pure Sn, Sn-0.7Cu, Sn-3.5Ag and Sn-3.8Ag-0.7Cu with or without UBMs.